Halogen Bonding

DOI: 10.1002/anie.201006781

Systematic Investigation of Halogen Bonding in Protein–Ligand Interactions**

Leo A. Hardegger, Bernd Kuhn, Beat Spinnler, Lilli Anselm, Robert Ecabert, Martine Stihle, Bernard Gsell, Ralf Thoma, Joachim Diez, Jörg Benz, Jean-Marc Plancher, Guido Hartmann, David W. Banner, Wolfgang Haap,* and François Diederich**

Halogen bonding (XB) refers to the noncovalent interaction of general structure DX···A between halogen-bearing compounds (DX: XB donor, where X = Cl, Br, I) and nucleophiles (A: XB acceptor).[1,2] Since the first observation in cocrystal structures of 1,4-dioxane and Br_2 by Hassel and Hvoslef in 1954,[3] XB has been widely used in crystal engineering and solid-state supramolecular chemistry.[4–6] The nature of the interaction and the underlying electronic prerequisite, the σ hole in the XB donor, have been the subject of extensive theoretical studies.[1,2,7–9] Most recently, the attractive nature of XB between 1-iodoperfluoroalkanes and various donors has also been demonstrated and quantified in solution studies.[10,11]

Novel inhibitors of human Cathepsin L (hCatL) were discovered[12] which bind covalently to the side chain of the catalytic Cys25 residue in the S1 pocket under formation of thioimidates, which are stabilized by the oxyanion hole of the protease. These ligands form hydrogen bonds to the backbone NH and C=O groups of Gly68 and Asp162, respectively, and fill the S2 and S3 pockets, thereby interacting with the enzyme through multiple lipophilic contacts. During the course of this research, we obtained an indication of an XB contact between a 4-chlorophenyl moiety of a ligand, whose binding affinity was enhanced by a factor of 13 compared to the unsubstituted phenyl derivative, and the backbone C=O group of Gly61 in the S3 pocket (Figure 1). This finding stimulated the preparation of compounds (−)-**1** to (−)-**40** (Table 1), which were subjected to a comprehensive investigation of XB in a biological environment.

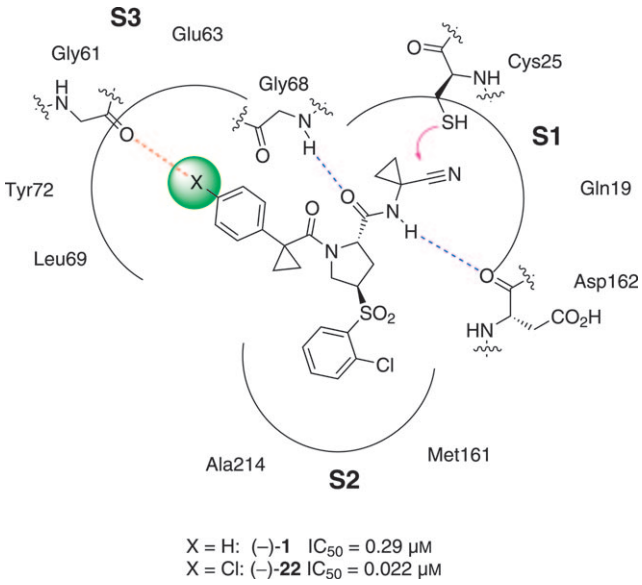

Figure 1. Binding mode of covalent inhibitors at the active site of hCatL with its three pockets. The substituent at position 4 of the phenyl ring in the S3 pocket, which approaches the C=O group of Gly61, is highlighted in green. If X = Cl, Br, or I, XB (red dashed line) with the backbone carbonyl oxygen atom of Gly61 increases the binding affinity.

The synthesis of the inhibitors is depicted in Scheme 1 (for details, see the Supporting Information). Enantiopure 4-hydroxyproline derivative (2*S*,4*S*)-**41** was transformed into thioether (2*S*,4*R*)-**42**, which was oxidized to the corresponding sulfone and subsequently saponified. The resulting acid was coupled with 1-aminocyclopropanecarbonitrile hydrochloride to afford amide (2*S*,4*R*)-**43**. Deprotection of the N atom (→(2*S*,4*R*)-**44**) and amide coupling with α-aryl acids **45** (see the Supporting Information) afforded the target molecules (2*S*,4*R*)-**46**. A second ligand class with a 2-chloro-4-(2,2,2-trifluoroethoxy)phenylsulfonyl moiety instead of 2-chlorophenylsulfonyl was also prepared and investigated (see the Supporting Information).

In both ligand classes, the aryl ring in the S3 pocket was substituted with H, Me, F, Cl, Br, I, and CF_3 groups to probe the importance of XB interactions with the C=O group of Gly61 in the S3 pocket. The aryl moiety was either a phenyl,

[*] L. A. Hardegger, Prof. Dr. F. Diederich
Laboratorium für Organische Chemie, ETH Zürich
Wolfgang-Pauli-Strasse 10, HCI, 8093 Zürich (Switzerland)
Fax: (+41) 44-632-1109
E-mail: diederich@org.chem.ethz.ch
Dr. B. Kuhn, B. Spinnler, L. Anselm, R. Ecabert, M. Stihle, B. Gsell, Dr. R. Thoma, Dr. J. Benz, Dr. J.-M. Plancher, Dr. G. Hartmann, Dr. D. W. Banner, Dr. W. Haap
F. Hoffmann-La Roche AG
Grenzacherstrasse 124, Bau 92, 4070 Basel (Switzerland)
Fax: (+41) 61-688-8714
E-mail: david.banner@roche.com
wolfgang.haap@roche.com
Dr. J. Diez
Expose GmbH, Grabenstrasse 11, 5313 Klingnau (Switzerland)

[**] This work was supported by a Novartis scholarship to L.A.H., a grant from the ETH Research Council, and F. Hoffmann-La Roche AG, Basel. We thank Dr. B. B. Bernet for proofreading and Dr. M. Stahl and Dr. H. Mauser for helpful discussions.

Supporting information for this article is available on the WWW under http://dx.doi.org/10.1002/anie.201006781.

Table 1: Covalent inhibitors of hCatL.[a]

X		H	Me	F	Cl	Br	I	X
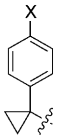	IC_{50}	(−)-**1** 0.29	(−)-**15** 0.13	(−)-**18** 0.34	(−)-**22** 0.022	(+)-**34** 0.012	(+)-**38** 0.0065	(−)-**40** 0.095
	log *D*	2.11	2.57	2.36	2.73	2.96	3.23	3.12
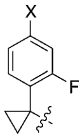	IC_{50}	(−)-**2** 0.32		(−)-**19** 0.35	(+)-**23** 0.030	(+)-**35** 0.0065	(+)-**39**[b] 0.0043	
	log *D*	1.98		2.02	2.63	2.75	3.00	
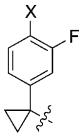	IC_{50}	(−)-**3** 0.52		(−)-**20** 0.93	(−)-**24** 0.022	(+)-**36**[b] 0.030		
	log *D*	2.37		2.46	2.98	3.08		
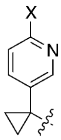	IC_{50}	(−)-**4** 1.48			(−)-**25** 0.25	(+)-**37** 0.14		
	log *D*	0.85			1.69	1.85		
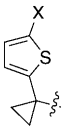	IC_{50}	(−)-**5** 0.16	(−)-**16** 0.41		(−)-**26** 0.16			
	log *D*	2.03	2.49		2.89			
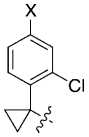	IC_{50}	(+)-**6** 0.69		(+)-**21** 0.36	(+)-**27** 0.022			
	log *D*	2.22		2.45	3.0			
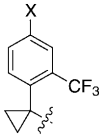	IC_{50}	(−)-**7** 0.88			(2*S*,4*R*)-**28** 0.055	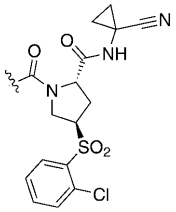		
	log *D*	2.51			2.98			
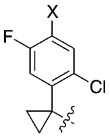	IC_{50}	(+)-**8** 0.30			(+)-**29** 0.023			
	log *D*	2.42			3.19			
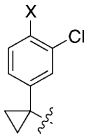	IC_{50}	(−)-**9** 0.34			(+)-**30** 0.032			
	log *D*	2.7			3.35			
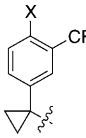	IC_{50}	(−)-**10** 0.46			(−)-**31** 0.18			
	logD	2.94			3.38			
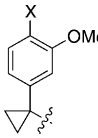	IC_{50}	(−)-**11** 0.52	(+)-**17** 0.22					
	log D	2.14	2.82					

pyridine, or thiophenyl ring with one or two additional substituents, such as F, CF_3, or Cl (Table 1, as well as Table 1SI in the Supporting Information).

The IC_{50} values for binding to hCatL were determined in a fluorescence assay by detecting the change in emission intensity caused by hCatL-mediated cleavage of the substrate Z-Val-Val-Arg-AMC (for definitions and details, see the Supporting Information).

The binding affinity of both ligand classes changed, as expected, for XB interactions as a function of the substituent at position 4 of the aryl ring. For example, the IC_{50} values in the series of 4-substituted phenyl derivatives (Table 1) remained essentially unchanged when moving from (−)-**1** (X = H; 0.29 μM) to (−)-**18** (X = F; 0.34 μM), as the fluorine substituent is not able to engage in σ-hole bonding. In contrast, the IC_{50} values decreased for the heavier halogens, in correlation with increasing XB donor strength, to 0.022 μM ((−)-**22**, X = Cl), 0.012 μM ((+)-**34**, X = Br), and 0.0065 μM ((+)-**38**, X = I). The binding affinity in ligand class 1 (Table 1) on changing from H to Cl increases by a factor of 12 ± 9 for all the substitution patterns in Table 1. Assuming competitive inhibition, this increase corresponds to a gain in the binding free enthalpy of $-\Delta\Delta G = 1.5 \pm 1.3$ kcal mol^{-1}.[13] In ligand class 2 (Table S1), a medium gain in binding affinity of 14 ± 20 is found on changing from H to Cl; this gain corresponds to a gain in binding free enthalpy of $-\Delta\Delta G = 1.5 \pm 1.8$ kcal mol^{-1} for competitive inhibition.

The IC_{50} values further decreased by a factor of approximately 2 and 4, respectively, upon changing the 4-position to Br or I. Thus, the I-substituted compound (+)-**39** (IC_{50} value: 0.0043 μM) is the most active inhibitor of the entire ligand class. A methyl substituent (compounds (−)-**15** to (+)-**17**), which is most similar in size to Cl, does not enhance the binding affinity significantly. A sur-

Table 1: (Continued)

X		H	Me	F	Cl	Br	I	X
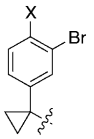		(−)-**12**						
	IC_{50}	0.52						
	log *D*	2.86						
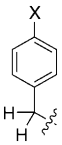		(−)-**13**			(−)-**32**			
	IC_{50}	0.97			0.56			
	log *D*	1.62			2.48			
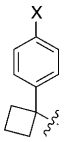		(−)-**14**			(−)-**33**			
	IC_{50}	0.39			0.024			
	log *D*	2.48			> 3.0			

[a] Top row: compound number; middle row: IC_{50} values (μM); bottom row: log *D* values. Compounds of the second ligand class show similar behavior. For details of the determination of IC_{50} and log *D* values, see the Supporting Information. The IC_{50} values were obtained from two or three measurements and have an uncertainty on average of 2–30%. [b] The IC_{50} values were obtained from eight measurements.

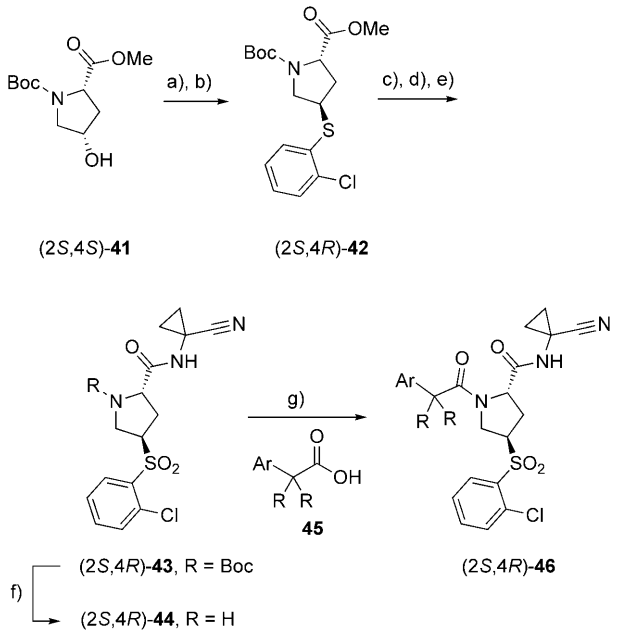

Scheme 1. Synthesis of target molecules (2*S*,4*R*)-**46**: a) 3-nitrobenzene-1-sulfonyl chloride (Nos-Cl), Et_3N, CH_2Cl_2, 0→22 °C, 10 h; b) 2-chlorobenzenethiol, Et_3N, propionitrile, 100 °C, 5.5 h, 90% (2 steps); c) *m*CPBA, CH_2Cl_2, 0→22 °C, 68 h; d) LiOH, THF/H_2O (1:1.5), 22 °C, 1.5 h; e) HATU, iPr_2EtN, 1-aminocyclopropanecarbonitrile hydrochloride, DMF, 22 °C, 14.5 h, 79% (3 steps); f) HCO_2H, 22 °C, 2.5 h, 80%; g) HATU, iPr_2EtN, amine (2*S*,4*R*)-**44**, DMF, 22 °C. Alternatively: $SOCl_2$, CH_2Cl_2, then iPr_2EtN, amine (2*S*,4*R*)-**44**, CH_2Cl_2, 22 °C. For substituents Ar and R, see Table 1 and Table 1SI. *m*CPBA: *meta*-chloroperbenzoic acid; HATU: *O*-(7-azabenzotriazol-1-yl)-*N*,*N*,*N*′,*N*′-tetraethyluronium hexafluorophosphate; Boc: *tert*-butyloxycarbonyl.

prisingly strong affinity was found in one case for a CF_3-substituted ligand ((−)-**40**; IC_{50} value: 0.095 μM).

It is important to note that the gain in binding affinity upon replacement of X = H by X = Cl or higher halides presumably does not arise from XB only. While the Cl substituent of (−)-**22** (Figure 2a) clearly forms the shortest contact to the backbone carbonyl oxygen atom of Gly61 (3.1 Å), three additional interactions to CH groups (Glu63 C_γ, Gly68 C_α, Tyr72 $C_{\varepsilon 2}$) at distances between 3.7 and 4.1 Å are made with the Cl atom. Moreover, the energetics of the stacking interaction of the aryl ring with the planar peptide fragment Gly67–Gly68, at the bottom of the S3 pocket, might be altered by changing X. There is no correlation between the log *D* value (logarithmic distribution coefficient octanol/water at pH 7.4) and the binding affinity (see Section 4 in the Supporting Information). While it can be expected that the C=O group of Gly61 is solvated in the apo structure, the replacement of water cannot explain the large gain in binding upon introducing Cl or heavier halides compared to F or Me substituents. Substitution of the 4-X-phenyl ring by one or even two additional electron-withdrawing substituents (as in (+)-**29**) resulted in only a small effect on binding affinity. Higher substitution patterns would have been desirable, but were not compatible with the ligand synthesis employed.

Much insight into the nature of XB interactions in the S3 pocket of hCatL was gained when a series of four X-ray cocrystals was solved (Figure 2). The X-aryl moieties stack, as expected, on the peptide backbone of Gly67–Gly68 and orient the X substituent towards the C=O group of Gly61. The Cl substituent in bound chlorophenyl derivative (−)-**22** (1.45 Å resolution, PDB code: 2xu1; Figure 2a and Figure 3SI) shows a nearly ideal XB interaction, with the O···Cl distance (3.1 Å) below the sum of the van der Waals radii (3.27 Å)[14] and the angle O···Cl–C (174°) close to 180°. For electrostatic reasons, XB is especially sensitive to the O···X–C angle, which should be close to 180°.[2,7,8,15–17] There are four independent protein–ligand complexes in the unit cell, for which we take the observed distances and angles as independent measurements and use the average (d(O···Cl) = 3.08 ± 0.11 Å; angle O···Cl–C = 173.6 ± 1.1°; see Section 5.1 in the Supporting Information).

The 5-chlorothiophen-2-yl derivative (−)-**26** (IC_{50} value: 0.16 μM) did not show stronger binding than the unsubstituted control compound (−)-**5** (IC_{50} value: 0.16 μM). The reason became apparent when the cocrystal structure of (−)-**26** with hCatL was solved (0.9 Å resolution, PDB code: 2xu3; Figure 2b and Figure 4SI). Two different conformations of the ligand were observed. In the conformer populated by 75%, the geometry is rather favorable for an XB interaction (d(O···Cl) = 3.1 Å; angle O···Cl–C = 166°). However, this gain in interaction energy seems to be compensated by intramolecular ligand strain, as indicated by a short, repulsive contact (3.0 Å) between the thiophenyl C atom attached to the cyclopropyl ring and the unsubstituted C atom adjacent to

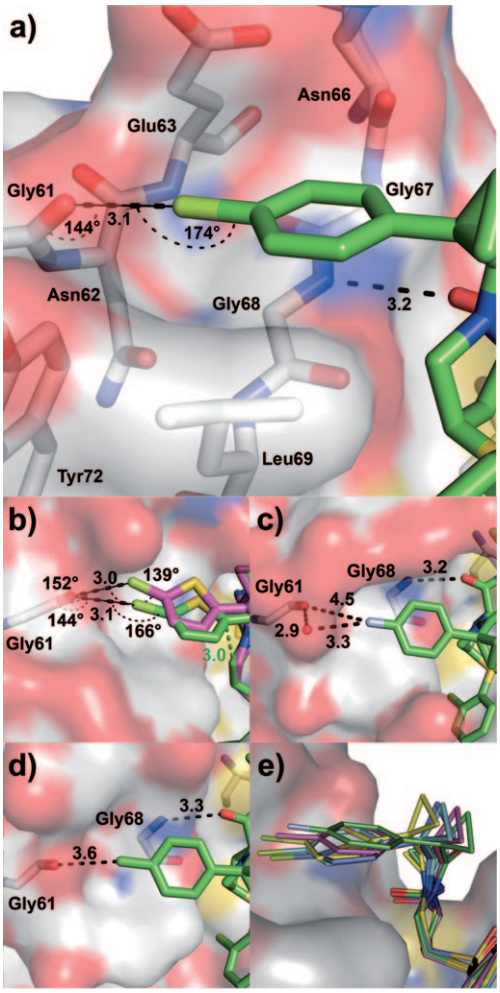

Figure 2. a) Cocrystal structure of (−)-**22** with hCatL at 1.45 Å resolution (PDB code: 2xu1). The amino acids of the S3 pocket are highlighted, as well as the XB interaction between the backbone carbonyl group of Gly61 and the chlorine atom. b) The cocrystal structure of (−)-**26** in a complex with hCatL at 0.9 Å resolution (PDB code: 2xu3) shows two different binding modes: 75% (green) undergo XB but suffer from intramolecular repulsion (green dashed line), 25% (pink) bind without apparent intramolecular strain, but undergo poorer XB. c) Cocrystal structure of (−)-**18** with hCatL at 1.12 Å resolution (PDB code: 2xu4). The repulsion between the carbonyl oxygen atom and the fluorine atom as well as the distances to the bridging water are highlighted. d) Cocrystal structure of (−)-**15** with hCatL at 1.6 Å resolution (PDB code: 2xu5). Distances are given in Å. Color code: C: gray (enzyme), green or pink (inhibitor); O: red; N: blue; S: yellow; Cl: lemon; F: light blue. e) Overlay of (−)-**15** (magenta), (−)-**18** (green), (−)-**22** (turquoise), and the two binding modes of (−)-**26** (yellow with strong XB, violet with weak XB). The adjustment of the phenyl moiety in the S3 pocket is accommodated by a slight change of the puckering of the five-membered ring.

the pyrrolidine N atom (green dashed line in Figure 2b). The second conformer, populated by 25%, features a much less favorable geometry for XB interactions (angle O···Cl–C = 139° at d(O···Cl) = 3.0 Å), but shows no apparent intramolecular strain. According to quantum-mechanical energy profile calculations (see below), the difference in the XB interaction energy for the two geometrical arrangements should be approximately 1 kcal mol^{-1} (Figure 9SI). An unfavorable O···Cl–C alignment is most probably also at the origin of the low affinity of chlorophenyl derivative (−)-**9** (IC_{50} value: 0.34 μM) compared to (−)-**22** (IC_{50} value: 0.022 μM).

The cocrystal structure of 4-fluorophenyl derivative (−)-**18** in a complex with hCatL (1.12 Å resolution, PDB code: 2xu4; Figure 2c and Figure 5SI) strongly confirms earlier reports that organofluorine substituents avoid regions of high electron density and avoid pointing directly at the O atoms of peptidic C=O bonds.[18] The F atom is moved away from the carbonyl group to avoid electrostatic repulsion, resulting in a O···F distance of 4.5 Å (sum of the van der Waals radii: 2.99 Å),[14] with a water molecule bridging this contact.

The methyl group in the cocrystal structure of (−)-**15** with hCatL (1.6 Å resolution, PDB code: 2xu5; Figure 2d and Figure 6SI) points toward the C=O group, but has a considerably longer O···C distance (3.6 Å) compared to the Cl derivative. Interestingly, the S3 pocket is widened through side chain shifts of Glu63, Leu69, and Tyr72 compared to the Cl structure, thus resulting in reduced interaction of the methyl group with the protein.

An overlay of all four crystal structures (Figure 2e and Figure 7SI) shows the unique mechanism that allows these adaptations of the X-aryl moiety in the S3 pocket. While all four ligands maintain identical binding geometries in the S1 and S2 pocket, the puckering of the central pyrrolidine ring in the ligands changes slightly. This does not involve much change in the conformational energy or in the intermolecular interactions in this region of the protein. This small change in the puckering of the five-membered ring, however, translates into larger differences in the penetration of the X-aryl moiety into the S3 pocket.

We compared our experimental results with the energetics of an isolated C=O···X-Phe interaction. Thus, we performed quantum mechanical calculations at an adequate theoretical level (MP2/aug-cc-pVDZ//B3LYP/aug-cc-pVDZ, for details see the Supporting Information) to determine interaction energy curves for different monosubstituted phenyl derivatives with *N*-methylacetamide. Model geometries were constrained to the relative orientation found in the X-ray complex structure of compound (−)-**22**. In line with previous calculations of related, unconstrained model systems,[8] we find attractive energy profiles for Cl, Br, and I, with a common minimum distance of 3.1 Å and well depths of −1.3, −2.2, and −3.5 kcal mol^{-1}, respectively (Figure 3, Figure 8SI). The observed O···Cl distance of 3.1 Å in the complex structure of (−)-**22** is close to its optimal value, further supporting a stabilizing effect of the XB interaction in the complex of the Cl derivative. XB interactions with the Br and especially I analogues should be stronger, which is reflected in the approximately two- and fourfold lower IC_{50} values for hCatL binding.

In contrast to the heavier halides, the interaction of the fluorine derivative is repulsive in nature, and the energy curve shows no minimum. The loss of binding affinity and the change in binding mode to a much larger intermolecular distance are in good agreement with this. The computed interaction energies for a close to linear arrangement are even

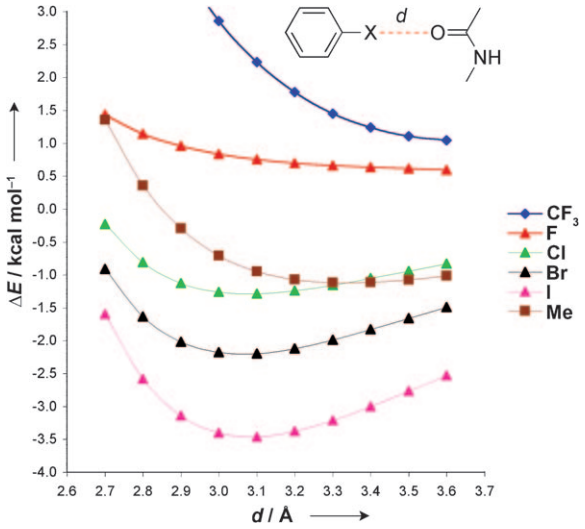

Figure 3. Calculated interaction energies for monosubstituted phenyl derivatives with *N*-methylacetamide as a peptide backbone mimic. Torsional angles from the crystal structure of (−)-**22** were applied as constraints to enforce the relative orientation at the active site of hCatL (see the Supporting Information).

more unfavorable with the CF_3 derivative. We expect that the binding mode will be different from the chlorine compound and that the good binding affinity of (−)-**40** (IC_{50} value: 0.095 μM) is due to intermolecular interactions of the CF_3 group that are unrelated to the C=O group of Gly61. Weak O···H−C interactions play a role for the methyl derivative, and the calculations predict a slightly weaker interaction energy than the chlorine derivative with the carbonyl oxygen atom at the observed distances. However, this difference in "solvation" is too small to fully explain the sixfold higher IC_{50} value of the methyl derivative. Widening of the S3 pocket and fewer intermolecular interactions are seen in the crystal structure of the methyl derivative, thus suggesting that the methyl substituent is less well accommodated in this "CH-rich" region, compared to the more polarizable Cl atom. Apparently, both a favorable XB interaction and an excellent general fit to the S3 pocket of hCatL contribute to the increases in the affinity of the non-fluorine-containing halide compounds.

In summary, we have presented the first systematic study on XB in protein–ligand complexes and show that XB can indeed serve as a powerful tool, comparable to hydrogen bonding, to enhance the binding affinity and certainly also affect the binding selectivity, as proven recently[19] in biological molecular recognition (for earlier examples of potential XB in biological complexes, see Section 7 of the Supporting Information). Our study confirms several theoretical predictions and also the recent results on model systems. XB increases in strength with the mass of the halide substituent (Cl < Br < I) but is non-existent with organofluorine compounds. The interaction has high geometrical requirements, such as a distance between the interacting atoms below the sum of the van der Waals radii and a strong dependence on the O···X−C angle. Establishing a halogen bond might enhance protein–ligand interactions by a factor of as much as 74 ((−)-**2** versus (+)-**39**), which translates into a gain in free enthalpy of $-\Delta\Delta G = 2.6$ kcal mol^{-1}. In view of this favorable energetic balance, it is predictable that XB will increasingly be used to enhance protein–ligand binding.

Received: October 28, 2010

Keywords: halogen bonding · medicinal chemistry · molecular recognition · protein–ligand interactions · structure–activity relationships

[1] P. Politzer, P. Lane, M. C. Concha, Y. Ma, J. S. Murray, *J. Mol. Model.* **2007**, *13*, 305 – 311.
[2] T. Clark, M. Hennemann, J. S. Murray, P. Politzer, *J. Mol. Model.* **2007**, *13*, 291 – 296.
[3] a) O. Hassel, J. Hvoslef, *Acta Chem. Scand.* **1954**, *8*, 873; b) O. Hassel, *Science* **1970**, *170*, 497 – 502.
[4] G. R. Desiraju, *Angew. Chem.* **1995**, *107*, 2541 – 2558; *Angew. Chem. Int. Ed. Engl.* **1995**, *34*, 2311 – 2327.
[5] a) P. Metrangolo, G. Resnati, *Chem. Eur. J.* **2001**, *7*, 2511 – 2519; b) P. Metrangolo, H. Neukirch, T. Pilati, G. Resnati, *Acc. Chem. Res.* **2005**, *38*, 386 – 395; c) P. Metrangolo, G. Resnati, *Halogen Bonding: Fundamentals and Applications*, Springer, Berlin, **2008**; d) P. Metrangolo, F. Meyer, T. Pilati, G. Resnati, G. Terraneo, *Angew. Chem.* **2008**, *120*, 6206 – 6220; *Angew. Chem. Int. Ed.* **2008**, *47*, 6114 – 6127; e) P. Metrangolo, G. Resnati, *Science* **2008**, *321*, 918 – 919.
[6] For some examples, see a) A. Sun, J. W. Lauher, N. S. Goroff, *Science* **2006**, *312*, 1030 – 1034; b) A. C. B. Lucassen, A. Karton, G. Leitus, L. J. W. Shimon, J. M. L. Martin, M. E. van der Boom, *Cryst. Growth Des.* **2007**, *7*, 386 – 392.
[7] J. P. M. Lommerse, A. J. Stone, R. Taylor, F. H. Allen, *J. Am. Chem. Soc.* **1996**, *118*, 3108 – 3116.
[8] a) K. E. Riley, K. M. Merz, Jr., *J. Phys. Chem. A* **2007**, *111*, 1688 – 1694; b) K. E. Riley, P. Hobza, *J. Chem. Theory Comput.* **2008**, *4*, 232 – 242.
[9] a) P. Politzer, J. S. Murray, P. Lane, *Int. J. Quantum Chem.* **2007**, *107*, 3046 – 3052; b) P. Politzer, J. S. Murray, T. Clark, *Phys. Chem. Chem. Phys.* **2010**, *12*, 7748 – 7757.
[10] R. Cabot, C. A. Hunter, *Chem. Commun.* **2009**, 2005 – 2007.
[11] M. G. Sarwar, B. Dragisic, L. J. Salsberg, C. Gouliaras, M. S. Taylor, *J. Am. Chem. Soc.* **2010**, *132*, 1646 – 1653.
[12] R. Alvarez Sanchez, D. Banner, S. M. Ceccarelli, U. Grether, W. Haap, P. Hartman, G. Hartmann, H. Hilpert, H. Kuehne, H. Mauser, J.-M. Plancher (F. Hoffmann-La Roche AG), US20100267722(A1), **2010**.
[13] Y.-C. Cheng, W. H. Prusoff, *Biochem. Pharmacol.* **1973**, *22*, 3099 – 3108.
[14] A. Bondi, *J. Phys. Chem.* **1964**, *68*, 441 – 451.
[15] K. E. Riley, J. S. Murray, P. Politzer, M. C. Concha, P. Hobza, *J. Chem. Theory Comput.* **2009**, *5*, 155 – 163.
[16] P. Auffinger, F. A. Hays, E. Westhof, P. S. Ho, *Proc. Natl. Acad. Sci. USA* **2004**, *101*, 16789 – 16794.
[17] C. Ouvrard, J.-Y. Le Questel, M. Berthelot, C. Laurence, *Acta Crystallogr. Sect. B* **2003**, *59*, 512 – 526.
[18] K. Müller, C. Faeh, F. Diederich, *Science* **2007**, *317*, 1881 – 1886.
[19] S. Baumli, J. A. Endicott, L. N. Johnson, *Chem. Biol.* **2010**, *17*, 931 – 936.

